Optimal Route Guidance and Model Predictive Control of Network-wide Traffic Emission

Deepak Ingole, Guilhem Mariotte, and Ludovic Leclercq

University of Lyon, IFSTTAR, ENTPE
Lyon 69120, France
{deepak.ingole, guilhem.mariotte, ludovic.leclercq}@ifsttar.fr

Short paper submitted for presentation at the hEART 2019 8th Symposium
September 4–6, 2019, Budapest, Hungary

Word count: 2980 words (excluding the references)
February 28, 2019

Abstract

In this paper, we propose optimal route guidance and Nonlinear Model Predictive Control (NMPC)-based gating control approach to reduce network-wide emission in an urban traffic network. An accumulation-based Macroscopic Fundamental Diagram (MFD) model of a single region city is developed to describe the evaluation of the traffic flows in a network. Moreover, a path flow distribution scheme using Dynamic User Equilibrium (DUE) discipline is designed to reproduce the driver's adaptation to controlled flow. The NMPC is developed to track the optimal green routing coefficients which will indirectly track the network-wide emission levels by manipulating the traffic flows into a region. Simulation results show the effectiveness of the proposed scheme in improving the traffic emissions inside and outside the perimeter. Comparative analysis of no control and NMPC shows that the proposed approach reduces emission by up to 13% as compared to the no control case.

Keywords: MFD; DUE; optimal green routing; emissions; NMPC.

1 Introduction

Emissions generated by vehicles in urban traffic areas, especially when traffic becomes congested and vehicles start to idle in long queues, significantly increase the level of harmful gases in the air such as Carbon Monoxide (CO) and Dioxide (CO_2), Hydrocarbon (HC), Nitrogen Oxides (NO_x), *etc.* (Choudhary and Gokhale, 2016, Mascia et al., 2017). On

top of emissions, traffic congestion leads to increased fuel consumption and its cost on the societies. There are several other impacts of traffic congestion and emissions, such as the increased travel time for the journey, public health issues, accidents, *etc.*

Vehicles are the dominant source of many air pollutant emissions in cities and congestion have the potential to significantly worsen ambient air quality, particularly near major highways. In recent years, significant efforts have been made to reduce the congestion by considering different control measures (such as traffic signal, ramp metering, speed control, route guidance, *etc.*) and perimeter control strategies (such as Proportional-Integral-Derivative (PID), MPC, optimal control *etc.*, see Kouvelas et al. (2017), Yang et al. (2017)). Most of the work in perimeter control domain considered the concept of MFD to model the traffic dynamics in the urban networks. The idea of behind the MFD was proposed by Godfrey (1969) and similar approaches were introduced later by Daganzo (2007), Geroliminis and Daganzo (2008).

There is a trivial solution to minimize emission: no vehicle should travel in the network. Optimal routing is certainly a more suitable solution as moving some vehicles from short path with high-level congestion to a longer one with higher speed can reduce emission. The optimal strategy should balance speed and distance as long paths may be counter prohibitive. However, optimal strategy will have some operational loss as it requires that people follow optimal guidance which means that some have to take longer routes should experience higher travel times. In this paper, we want to investigate the inherent control strategy trying to achieve optimal routing by controlling the flow of the different city gates. Selfish user discipline (DUE) will force some users to take urban freeways and go around the city center. Users will not require route guidance but the gating strategy will modify the travel time when crossing the city center and then modify the splitting coefficient between the city center and urban freeways for all Origin Destination (OD) pairs. The splitting coefficient is the estimated optimal splitting ratio of inflow demand between the freeway and regional route which minimize the network-wide emission.

In short, our network-wide emission control scheme is composed of two layers. The first layer (optimal green routing) determines for the next time horizon the optimal splitting coefficient (β^r) for all OD pairs (only two alternatives are possible for each OD, i.e., freeway or regional route). The second layer is an NMPC-based gating controller, which determine the flow limits that can enter the city at each time-step over the time horizon in order to DUE discipline distribute users among both alternatives to be as close as possible to the optimal splitting coefficient. The efficiency of the proposed scheme is demonstrated through a case study of a single region city and its performance is analyzed and compared with the no control case. Results indicate that the proposed scheme can significantly reduce network-wide emissions (NO_X and CO_2) and Total Time Spent (TTS), and increase mean speed in the region.

2 Network Modeling

2.1 The Network

The city network under consideration comprised of a homogeneous urban region with one internal regional route and six transferring regional routes. Each transferring route has an urban freeway alternative, as depicted in Fig. 1. In this study, a regional route, or simply "route" in the following, corresponds to the aggregation of multiple individual paths on the real city street network that shares some characteristics in common. All six transferring routes also include an Inbound Link (IL) at the region entry.

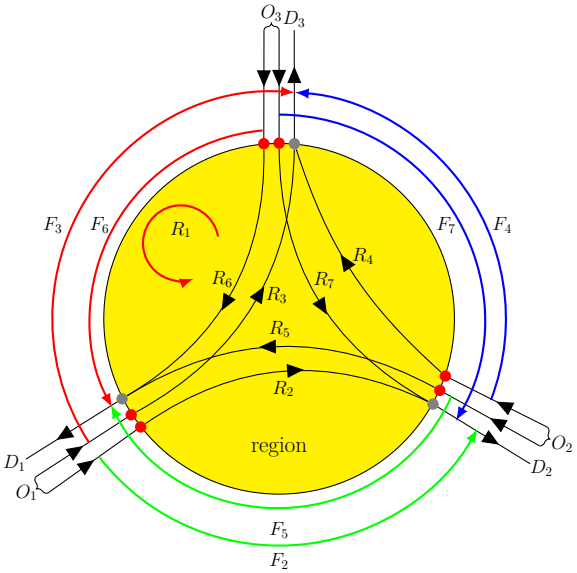

Figure 1: Single region network with one internal route (R_1), six external routes ($R_2, \ldots, R_7$), six urban freeways ($F_2, \ldots, F_7$), and six inflow controlled gates.

We assume that the traffic dynamics of the region is described by a well-defined production-MFD $P(n)$ (in [veh.m/s]), or equivalently, a speed-MFD $V(n)$ (in [m/s]), where n (in [veh]) is the total number of circulating vehicles in the region. The production-MFD is notably defined by the following characteristic values: jam accumulation n_j, critical accumulation n_c, maximum production or capacity $P_c = P(n_c)$, and free-flow speed $\tilde{v} = dP(0)/dn$. Each inbound link is described by a point-queue model, and each freeway is described by a conservation equation with a fixed delay (assumed to be always in free-flow conditions with constant mean speed).

2.2 MFD Traffic Model

In this work, we used the accumulation-based MFD model of the region with $\mathcal{R}$ regional routes of different lengths L_i. The accumulations n_i are the numbers of vehicles traveling

on each route R_i inside the region, satisfying the following system (Geroliminis, 2015, Mariotte and Leclercq, 2018):

$$\frac{dn_i}{dt} = q_{\text{in},i}(t) - q_{\text{out},i}(t), \qquad \forall i \in \{1, \dots, \mathcal{R}\}, \tag{1}$$

where $q_{\text{in},i}(t)$ and $q_{\text{out},i}(t)$ are respectively the effective inflow and outflow for route i.

In this work, we use the model of flow exchange at perimeter proposed by Mariotte and Leclercq (2018) to define $q_{\text{in},i}(t)$ and $q_{\text{out},i}(t)$. The effective inflow $q_{\text{in},i}(t)$ for a transferring route R_i is the result of the competition between a corresponding demand $\lambda_i(t)$ from the inbound link, an entry supply function $I_i(n_i, n)$ that mimic the congestion in the region reaching the entry, and a gating inflow $u_i^\star(t)$ given by the NMPC. The inflow of the internal route is assumed to be unrestricted, thus equal to its demand:

$$q_{\text{in},i}(t) = \begin{cases} \min(\lambda_i(t), I_i(n_i(t), n(t)), u_i^\star(t)), & \forall i \geq 2, \\ \lambda_i(t), & i = 1, \end{cases} \tag{2}$$

The effective outflow $q_{\text{out},i}(t)$ for a transferring route R_i is the result of the competition between its corresponding demand function $O_i(n_i, n)$ representing the region dynamics, and an eventual exogenous limitation $\mu_i(t)$ representing some bottleneck at the exit of the route. As in Mariotte and Leclercq (2018), we assume the demand function to be maximum in oversaturated conditions for the transferring routes: $O_i(n_i, n) = n_i/n \times P_c/L_i$ for $n > n_c$. For the internal route $i = 1$, the outflow is supposed unrestricted and described by a decreasing function when $n > n_c$ to mimic internal congestion: $O_1(n_1, n) = n_1/n \times P(n)/L_1$. Then, the effective outflows for both internal and transferring routes are calculated with the following relationships (Mariotte and Leclercq, 2018):

$$q_{\text{out},k}(t) = \min(\mu_k(t), O_k(n_k, n)), \tag{3}$$

where $k = \arg\min_{1 \leq i \leq N} \frac{\mu_i}{O_i(n_i,n)}$ and

$$q_{\text{out},i}(t) = \frac{n_i(t)}{n_k(t)} \frac{L_k}{L_i} q_{\text{out},k}(t), \qquad \forall i \neq k. \tag{4}$$

3 Routing Discipline and Emission Calculations

3.1 User Equilibrium Discipline

The users willing to enter route R_i ($i \geq 2$) can choose to take the urban freeway (F) instead of entering the IL and crossing the region to reach their destination. We assume

that these travelers are making their choices according to DUE as follow:

$$\begin{cases} T_{IL_i}(t) + T_{R_i}(t + T_{IL_i}(t)) < T_{F_i} \Leftrightarrow \begin{array}{l}\text{no one}\\ \text{chooses}\\ \text{the freeway,}\end{array} \\ T_{IL_i}(t) + T_{R_i}(t + T_{IL_i}(t)) = T_{F_i} \Leftrightarrow \begin{array}{l}\text{at least one}\\ \text{user chooses}\\ \text{the freeway,}\end{array} \end{cases} \tag{5}$$

where T_{F_i} is the freeway free-flow travel time, $T_{IL_i}(t)$ and $T_{R_i}(t)$ are the exact predictive travel times on the IL and in the region, respectively, for route R_i. The IL is assumed to have a total length L_{IL_i}, and to consist of two parts: the first one is free-flow with speed $\tilde{v}_{IL_i}$, and the second one is congested, dynamically represented by a point-queue model. Thus its travel time consists of two terms: $T_{IL_i}(t) = L_{IL_i}/\tilde{v}_{IL_i} + \delta_{IL_i}(t + L_{IL_i}/\tilde{v}_{IL_i})$, where $\delta_{IL_i}(t)$ is the exact predictive delay in the IL.

Both $\delta_{IL_i}(t)$ and $T_{R_i}(t)$ are the result of traffic dynamics that will be observed inside the region after t. During the simulation, because we do not know the future evolution of the system at t, we choose to estimate these values based on the current state observation:

$$T^*_{R_i}(t) = L_i/V(n(t)), \tag{6}$$
$$\delta^*_{IL_i}(t) = n_{IL_i}(t)/q_{\text{in},IL_i}(t - dt). \tag{7}$$

where $n_{IL_i}(t)$ is the accumulation and $q_{\text{in},IL_i}(t - dt)$ is the effective inflow into the IL i, estimated from the previous time step $t - dt$ as we do not know it at t. Then, the estimation $T^*_{IL_i}(t)$ of the IL predictive travel time is directly obtained with $\delta^*_{IL_i}(t)$.

For a given route i, switching the users to the freeway F_i is achieved by splitting the inflow demand $\lambda_i(t)$ into the IL inflow $q_{\text{in},IL_i}(t)$ and the freeway inflow $q_{\text{in},F_i}(t)$ as follow:

Case 1 If $T^*_{IL_i}(t) + T^*_{R_i}(t) < T_{F_i}$, users switch to the regional route:

$$\gamma_i(t) = b_i.q_{\text{in},F_i}(t - dt)/\lambda_i(t - dt) \tag{8a}$$
$$q_{\text{in},IL_i}(t) = (1 - \gamma_i(t))\lambda_i(t) \tag{8b}$$
$$q_{\text{in},F_i}(t) = \gamma_i(t)\lambda_i(t) \tag{8c}$$

Case 2 Otherwise, users switch to the freeway:

$$\gamma_i(t) = b_i.q_{\text{in},F_i}(t - dt)/\lambda_i(t - dt) + b_i \tag{9a}$$
$$q_{\text{in},IL_i}(t) = \max\left((1 - \gamma_i(t))\lambda_i(t); q^{\min}_{\text{in},IL_i}\right) \tag{9b}$$
$$q_{\text{in},F_i}(t) = \lambda_i(t) - q_{\text{in},IL_i}(t) \tag{9c}$$

The inflow splitting coefficient $\gamma_i(t) \in [0, 1]$ corresponds to the proportion of users on path i who just took the freeway alternative F_i to reach their destination and b_i in [0,1] is a smoothing parameter.

Then, the accumulation in each IL_i is governed by the following conservation equation:

$$\frac{dn_{IL_i}}{dt} = q_{\text{in},IL_i}(t) - q_{\text{out},IL_i}(t), \tag{10}$$

where the outflow is equal to the inflow in route i, i.e., $q_{\text{out},IL_i}(t) = q_{\text{in},i}(t)$. Traffic dynamics on the freeway is represented with a fixed delay (the freeway free-flow travel time T_{F_i}) as:

$$\frac{dn_{F_i}}{dt} = q_{\text{in},F_i}(t) - q_{\text{in},F_i}(t - T_{F_i}). \tag{11}$$

3.2 Emission Model

We use emission macroscopic rules that provide the emission rate (in [g/km]) of a reference vehicle depending on the mean speed $v^*(t)$. These rules come from the COPERT IV framework (Ntziachristos et al., 2009) and have been integrated with the fourth-degree polynomial for simplicity (Lejri et al., 2018). We obtained the Emission Factor (EF) model of NO_x and CO_2 based on the reference emission data recorded for the speed profile of personal cars. Then, the evolution of emission level $E_{dt}(t)$ (in [g]) of one pollutant between t and $t + dt$ is calculated as:

$$E_{dt}(t) = EF(v^*(t)) \times n^*(t) \times v^*(t) \times dt, \tag{12}$$

where $EF(v^*(t))$ is the emission factor of the pollutant considered (in [g/km]), $n^*(t)$ the accumulation and $v^*(t)$ the mean speed at t. The emission factor $EF(v^*)$ is estimated through curve fitting technique applied to emission curves shown in Fig. 2. $E_{dt}(t)$ corresponds to instantaneous emissions because it is calculated for a small time step $dt = 1$ s. On route i in the region, $n^*(t)$ is the partial accumulation $n_i(t)$, and $v^*(t)$ is the region mean speed $v(t)$ and similarly, for the freeway and IL.

3.3 Optimal Green Routing

To reduce the network-wide emission, we need the trajectory of references for NMPC. The references for the NMPC is the optimal green routing splitting coefficient (β_i^r) for all OD pairs. The idea is to estimate a trajectory (for 60 s) of β_i^r which will minimize the network-wide emission. At time t, we estimate the optimal splitting ratio of inflow demand between freeway and region which will minimize the network-wide emission. Here we assume that the speed and accumulation on freeways and region (including IL) is constant for $[t, t+60]$ and it is the same as at t.

To find the values of (β_i^r), we solve the following Linear Programming (LP) problem with bounds:

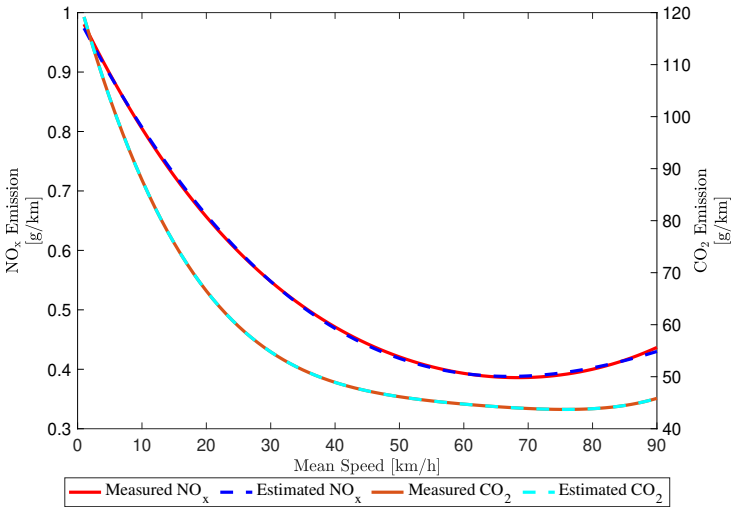

Figure 2: Reference and estimated emission factor of NO_x and CO_2 for varying mean speed.

$$\min_{\beta_i^r(t)} \int_t^{t+60} (EF(\tilde{v}_f(t))\beta_i^r(t)\lambda_i(t)L_f + EF(v(t))(1-\beta_i^r(t))\lambda_i(t)L_i + EF(v_{IL_i}(t))(1-\beta_i^r(t))\lambda_i(t)L_{IL_i})\, dt, \quad (13a)$$

subject to:

$$0 \leq \beta_i^r(t) \leq 1, \qquad \forall t \in [t, t+60], \;\; i = 2, \ldots, 7, \quad (13b)$$

where $EF(v(t)), EF(v_{IL})(t)$ and $EF(\tilde{v}_f)(t)$ are the NO_X emission factors for the regional route, IL, and freeway respectively. After obtaining the β_i^r trajectory, it is smoothed by Method of Successive Averages (MSA) as follows:

$$\beta_i^r(t) = \frac{1}{3}\beta_i^r(t) + \frac{2}{3}\beta_i^r(t - dt). \quad (14)$$

The value of output variable $\beta_i(t)$ is measured at the exit of the region with following relation:

$$\beta_i(t) = 1 - (q_{\text{out},i}(t)/\lambda_i(t)). \quad (15)$$

4 Nonlinear Model Predictive Control

4.1 Problem formulation

NMPC as a constrained finite-time optimal control problem for reference tracking is represented as (Grüne and Pannek, 2017, Chapter 1),

$$\min_{u_i(.)} \int_0^T \frac{1}{2} \left(||\beta_i(t) - \beta_i^r(t)||_Q^2 + ||\Delta u_i(t)||_R^2 \right) dt, \tag{16a}$$

subject to:

$$\dot{x_i}(t) = f(x_i(t), u_i(t)), \qquad \forall t \in [0, T], \tag{16b}$$
$$\Delta u_i(t) = u_i(t) - u_i(t-1), \qquad \forall t \in [0, T], \tag{16c}$$
$$u_{\min,i} \leq u_i(t) \leq u_{\max,i}, \qquad \forall t \in [0, T], \tag{16d}$$
$$\beta_i(t) \in [0, 1], \qquad \forall t \in [0, T], \tag{16e}$$
$$x_i(0) = \hat{x}_{i,0}, \tag{16f}$$
$$u_i(-1) = 0, \tag{16g}$$

where $x_i(t) \in \mathbb{R}^{n_x}$ denote the differential states, $\dot{x_i}(t)$ are the differential state derivatives, $\beta_i(t) \in \mathbb{R}^{n_y}$ are the outputs corresponding to splitting coefficient, and $\beta_i^r(t) \in \mathbb{R}^{n_y}$ are the references for optimal splitting coefficients, and $u_i(t) \in \mathbb{R}^{n_u}$ denote the control inputs at time t. The term (16a), is the cost function and $T > 0$ is the prediction horizon. The cost function is weighted by $Q \succeq 0$ and $R \succ 0$. The function f in (16b) describes the nonlinear dynamics of the traffic network under consideration which is as given by (1).

4.2 Implementation

The presented NMPC strategy based on the MFD model was implemented and synthesized in a MATLAB. The sample time of the 1 s is considered to measure the traffic states $(x_i(t))$ of the system whereas the optimal control actions $(u_i^\star(t)), i = 2, \ldots, 7$ and references $\beta_i^r(t), i = 2, \ldots, 7$ are updated at each 60 s. In the implementation of NMPC algorithm, prediction horizon, input penalty, and output penalty was set to 10, $0.001 \times \mathbb{I}_{(n_u \times n_u)}$, and $100 \times \mathbb{I}_{(n_y \times n_y)}$, respectively. The constraints on input flow rates $(u_i(t))$ was set to [0.1,6] veh/s.

5 Simulation Results

In order to demonstrate the effectiveness of the proposed scheme, a case study has been considered and the results are compared with the NoControl (NC) case. In the simulation, the values of the macroscopic traffic flow model parameters are given in the Table 1.

Table 1: Values of the MFD model parameters used in the case study.

Parameter	**Value**	**Unit**
Region trip lengths (L_i)	$[5\ 6\ 7\ 5.5\ 8\ 7.5\ 8.5]\times10^3$	m
Region maximum production (P_c)	150000	veh.m/s
Region free-flow speed ($\tilde{v}$)	14	m/s
Region jam accumulation (n_j)	60000	veh
Region critical accumulation (n_c)	12000	veh
Freeway trip length (L_f)	22500	m
Freeway free-flow speed ($\tilde{v}_f$)	14	m/s
Freeway free-flow travel time (T_f)	1428	s
IL free-flow speeds ($\tilde{v}_{IL_i}$)	19	m/s
IL trip lengths (L_{IL_i})	2500	m

Fig. 3 shows the inflow demand profiles of all routes used in case study.

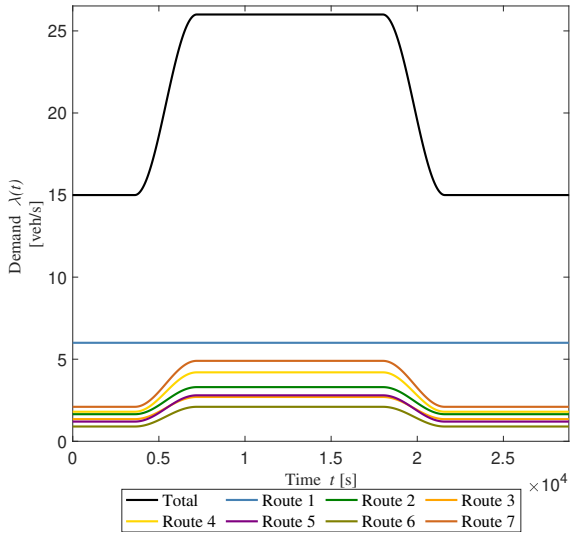

Figure 3: Traffic inflow demand profiles for all routes and its total.

As aforementioned, the objective of the controller is to track $\beta_i^r(t)$ reference trajectory while respecting the constraints on inflow rates. Fig. 4 shows the response of NMPC scheme while tracking $\beta_i^r(t)$ trajectories. For control case, during network loading period measured $\beta_i(t)$ values are zero as shown in the zoomed part of Fig. 4(a), during that time there was no outflow at the exit of the region. After that, there was a gradual increase in the outflows and decrease in the $\beta_i(t)$ values. The spike in the β_i was due to the first

outputs at the exit. However, it can be observed that in some parts especially during high inflow demands (from 3600-18000 s), $\beta_2(t), \ldots, \beta_5(t)$ values are not tracking to their references. This is due to the DUE discipline which enforces the limitation on the number of users. For the NC case, $\beta_i(t)$ values are oscillating during high congestion, except for the $\beta_4(t)$ which is due to the highest outflow and low accumulation on the R_4. For $\beta_7(t)$, reference values are oscillating between 0 and 1, which is because of the R_7 which have the longest trip length.

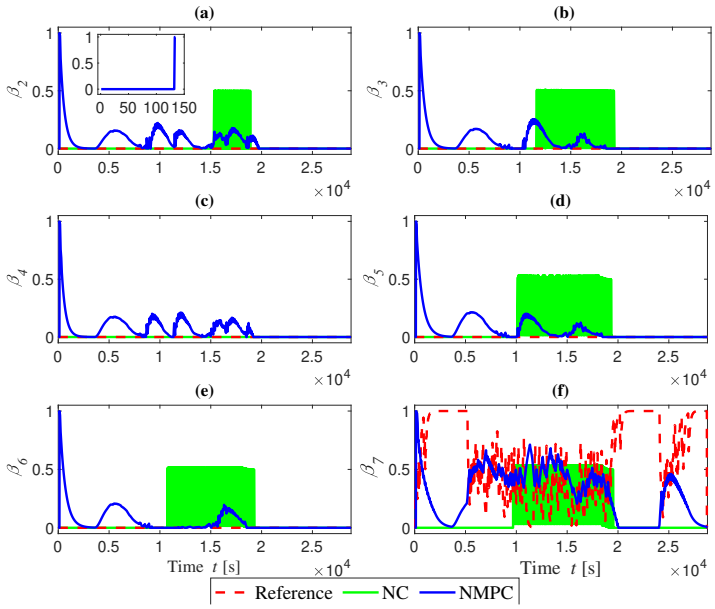

Figure 4: Performance evaluation of β_i coefficient.

Fig. 5 depicts the emission levels of NO_x and CO_2 and mean speed in the whole network (left column) and in the region (right column). Note here that CO_2 is only monitored and has no contribution to the calculation of $\beta_i(t)(t)$. It can be observed that with the NMPC scheme there is a significant decrease in the network-wide and region emissions and an increase in mean speeds. With NMPC, amount of NO_x is reduced by 329 kg and CO_2 by 22781 kg. It indicates that the proposed scheme is beneficial for perimeter area as well as in total.

Fig. 6 depicts the total emission levels of NO_x and CO_2 and mean speed on the IL (left column) and on the freeway (right column). With NMPC, on the ILs total (sum of IL_i) emissions are decreased and mean speed is increased. The oscillations in the mean speed are due to the inflow which is also oscillating (see Fig. 7(e)). As expected, with NMPC freeways have high emissions as compared to NC. This is due to the fixed mean speed on all the freeways.

Fig. 7 presents the total accumulation, inflow, and outflow inside the region (left column) and route-wise accumulation, inflow, and outflow inside the region (right column).

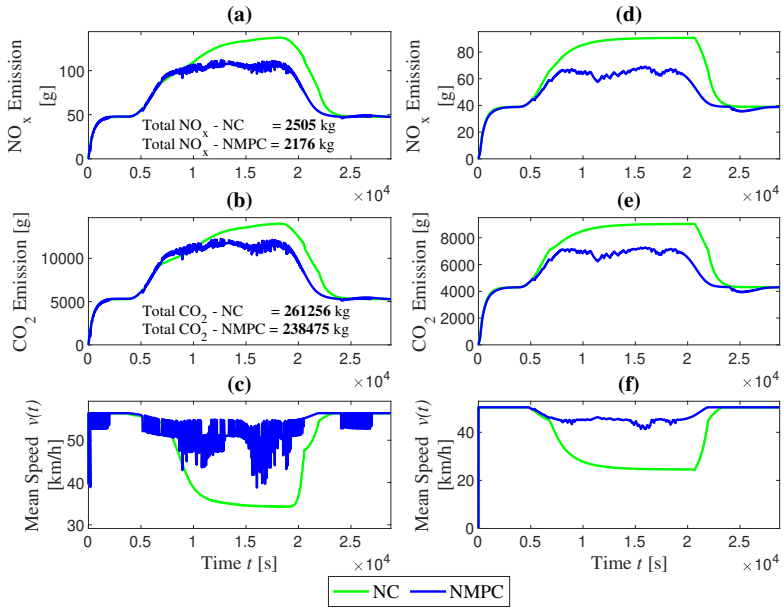

Figure 5: Performance evaluations of network-wide emissions and mean speed (left column) and region emission and mean speed (right column).

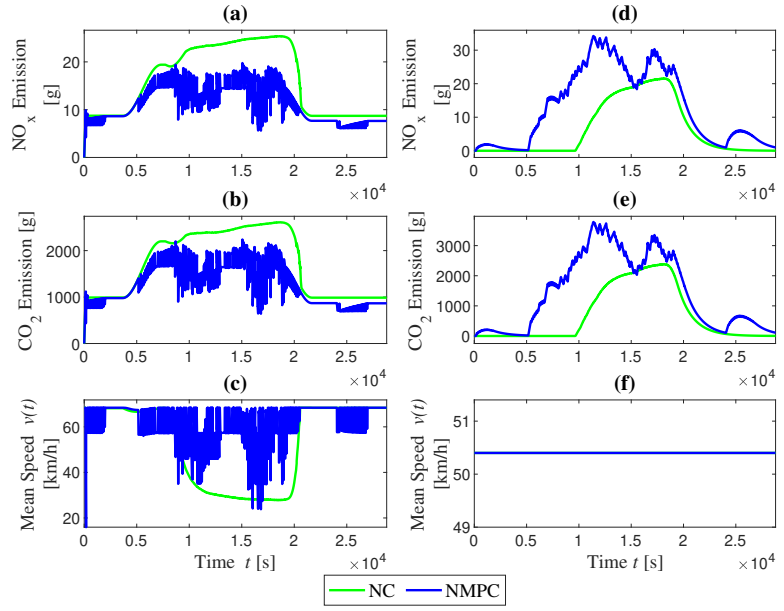

Figure 6: Response of total emissions and mean speed on the IL (left column) and freeway (right column).

It can be seen that during loading and unloading period the total accumulation inside the perimeter is almost similar in NC and NMPC case. Whereas during the high demand period, NC drives region in high congestion and NMPC keeps accumulation around the critical value which is almost similar to tracking total accumulation by the controller. This

is because of the improved inflow and outflow. The contribution of accumulation and flows in the total can be observed in the right column of the Fig. 7.

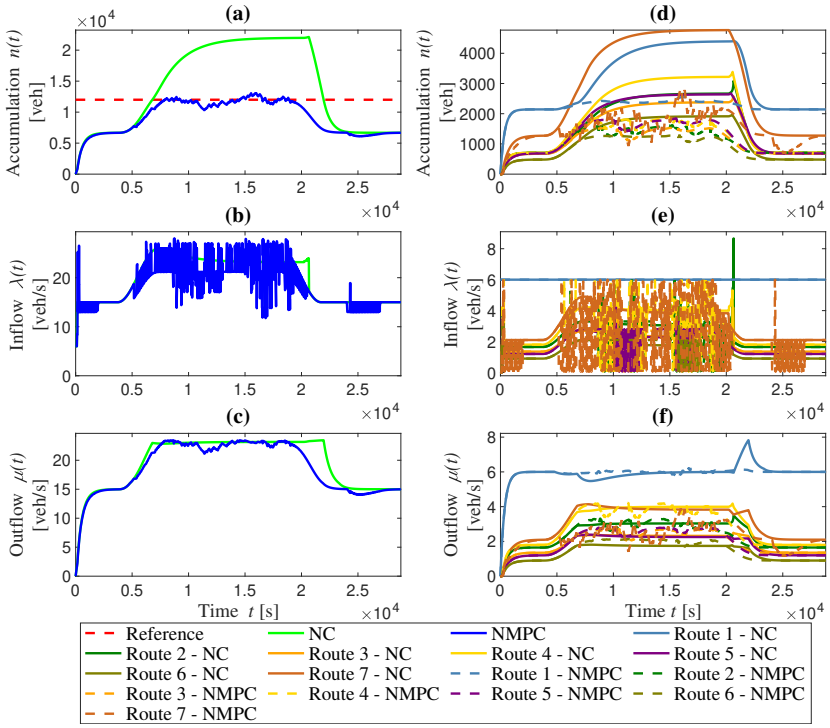

Figure 7: Response of total (left column) and route-wise (right column) accumulation, inflow, and outflow.

Fig. 8 shows the total TTS (sum of region, ILs, and freeways) in the network (a) and exit production of the network (b). It can be observed that the total TTS with NMPC is less which is better for the users to finish their trips in less time.

5.1 Comparative Analysis

Table 2 gives a summary of the performance evaluation of NC and NMPC schemes. Given values in the table are calculated for the whole simulation time (8 h) in the form of the percentage (%) with respect to the NC. The values indicated in red color shows a negative effect, and values in green color show a significant positive effect of the NMPC scheme. Table 2 shows the four performance indicators that are emission, TTS and mean speed in the region, inbound links, freeways, and whole network. The results indicate that NMPC scheme with optimal green routing is capable of improving green mobility in the network, as it shows a decreased amount of emissions (expect on freeways), TTS and mean speed, in comparison to the NC case. As expected freeways have high emissions due to a constant speed and long distance, but higher improvements in others parts compensate it which in

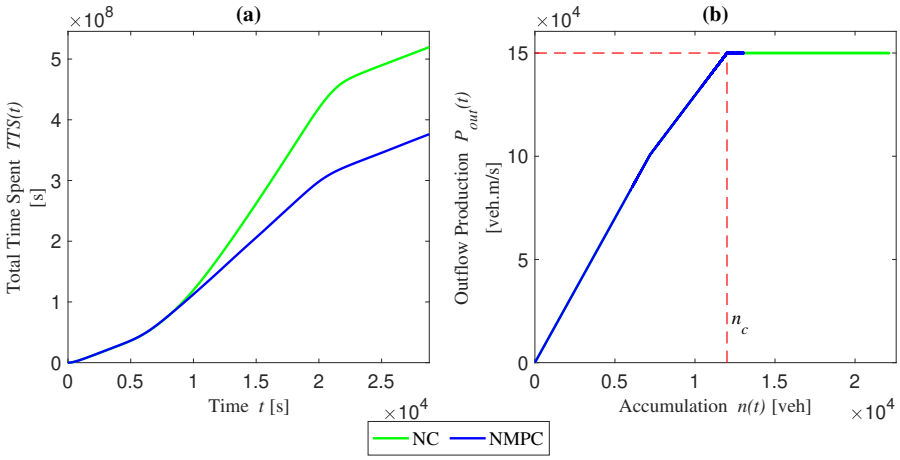

Figure 8: Response of TTS (a) and production MFD (b) at the exit.

Table 2: Performance comparison of nocontrol and NMPC gating control schemes.

Indicator	region	IL	Freeway	Total
Emission NO_x	-21.0	-25.50	109.7	-13.10
Emission CO_2	-16.85	-24.33	109.7	-8.72
TTS	-25.85	-30.50	-31.80	-25.0
Mean Speed	24.88	18.97	0	13.81

turn shows a decrease in network-wide emission.

6 Conclusions

We have proposed an approach to reduce network-wide emissions by using optimal green routing and NMPC-based gating control strategies. The NMPC strategy is developed based on an accumulation-based MFD model, along with that a DUE scheme is developed for the path distribution assuming the freeway option. Further, an optimal green routing scheme is proposed to find splitting coefficients which give the optimal route choice corresponding low emission route. The reference trajectories of the splitting coefficients are estimated and utilized in the NMPC scheme developed to track measured splitting coefficients. Performance of the developed approach is demonstrated through a single region urban network with routes, inbound links, and freeways. Simulation results show the

potential for significant improvement in network-wide emission, TTS, and mean speed. A further observation is that the proposed approach also helps to protect the region from severe congestion.

Acknowledgment

This project has received funding from the European Research Council (ERC) under the European Union's Horizon 2020 research and innovation program (grant agreement No 646592 – MAGnUM project).

References

Arti Choudhary and Sharad Gokhale. Urban real-world driving traffic emissions during interruption and congestion. *Transportation Research Part D: Transport and Environment*, 43:59–70, 2016.

Carlos F Daganzo. Urban gridlock: Macroscopic modeling and mitigation approaches. *Transportation Research Part B: Methodological*, 41(1):49–62, 2007.

Nikolas Geroliminis. Cruising-for-parking in congested cities with an MFD representation. *Economics of Transportation*, 4(3):156–165, 2015.

Nikolas Geroliminis and Carlos F Daganzo. Existence of urban-scale macroscopic fundamental diagrams: Some experimental findings. *Transportation Research Part B: Methodological*, 42 (9):759–770, 2008.

JW Godfrey. The mechanism of a road network. *Traffic Engineering & Control*, 8(8), 1969.

Lars Grüne and Jürgen Pannek. *Nonlinear Model Predictive Control : Theory and Algorithms. 2nd Edition*. Communications and Control Engineering. Springer, Cham, Switzerland, 2017.

Anastasios Kouvelas, Mohammadreza Saeedmanesh, and Nikolas Geroliminis. Enhancing model-based feedback perimeter control with data-driven online adaptive optimization. *Transportation Research Part B: Methodological*, 96:26–45, 2017.

Delphine Lejri, Arnaud Can, Nicole Schiper, and Ludovic Leclercq. Accounting for traffic speed dynamics when calculating copert and phem pollutant emissions at the urban scale. *Transportation research part D: Transport and Environment*, 63:588–603, 2018.

Guilhem Mariotte and Ludovic Leclercq. MFD-based simulation: Spillbacks in multi-reservoir networks. *97th Annual Meeting TRB, Washington D.C.*, 2018.

Margherita Mascia, Simon Hu, Ke Han, Robin North, Martine Van Poppel, Jan Theunis, Carolien Beckx, and Martin Litzenberger. Impact of traffic management on black carbon emissions: a microsimulation study. *Networks and Spatial Economics*, 17(1):269–291, 2017.

Leonidas Ntziachristos, Dimitrios Gkatzoflias, Chariton Kouridis, and Zissis Samaras. COPERT: a european road transport emission inventory model. In *Information technologies in environmental engineering*, pages 491–504. Springer, 2009.

Kaidi Yang, Nan Zheng, and Monica Menendez. Multi-scale perimeter control approach in a connected-vehicle environment. *Transportation Research Part C: Emerging Technologies*, 2017.